Inherited Continental Zircons in Oceanic Rocks – True or False

Anders Bjerga (anders.bjerga@gmail.com)
University of Bergen https://orcid.org/0000-0001-5541-3898
Håvard Stubseid
University of Bergen
Leif-Erik Pedersen
University of Bergen
Rolf Birger Pedersen
University of Bergen

Article

Keywords: Zircons, Oceanic, magmatic

Posted Date: August 11th, 2021

DOI: https://doi.org/10.21203/rs.3.rs-778290/v1

Version of Record: A version of this preprint was published at Communications Earth & Environment on February 23rd, 2022. See the published version at https://doi.org/10.1038/s43247-022-00372-2.

Abstract

Many studies have reported U-Pb dates of zircons that are older than the rocks that contain them, and they are therefore thought to be inherited from older rock complexes. Their presence has profound geodynamic implications and has been used to hypothesize about concealed micro-continents, continental crust beneath ocean islands, and recycling of continental material in the mantle beneath mid-ocean ridges. However, there is skepticism in the scientific community whether these zircons are truly inherited from crustal fragments or represent contaminants from sample preparation and processing. In this study, we combine single zircon U-Pb dates with structural radiation damage determined by Raman spectroscopy from a Pliocene mid-ocean ridge gabbro and show that the thermal history of Precambrian zircons found in the sample contradicts an inherited origin. To confirm that our approach allows distinction between contamination and true inherited zircons, we investigated igneous rocks that formed during the opening of the Atlantic Ocean and find that the calculated radiation damage age of old inherited grains corresponds with the crystallization dates of the young magmatic zircons.

Introduction

Inherited zircons ($ZrSiO_4$), displaying U-Pb dates older than their host-rock, are a common feature of felsic rocks and are increasingly being reported from mafic and ultramafic rocks from both oceanic[2-8] and continental[9-15] environments. While the ability to inherit older zircons in continental settings remains indisputable, reports suggesting that zircons can survive and retain their U-Pb dates under certain chemical conditions in the mantle[10, 16, 17] indicate that zircons may be recycled through the mantle and therefore appear in mantle peridotites or mantle-derived igneous rocks. However, experimental studies show that zircons undergo rapid dissolution in mafic melts raising questions about the true origin of zircon in these settings[18-21]. During investigations of a gabbro sampled from a peridotite-gabbro complex in the Mohn's ridge (Figure 1), we recovered several zircons using conventional mineral separation. For zircons produced by the gabbroic magma, we expected dates between 3 and 5 Ma, consistent with magnetic anomalies and seafloor spreading rates. For some of these zircons, Precambrian dates were obtained, significantly older than anticipated, with the oldest grain having a $^{207}Pb/^{235}U$ date of 2724 Ma. If these zircons are derived from recycled continental material in the sub-oceanic mantle source of the peridotite-gabbro complex, it clearly has significant geodynamic implications.

Because the risk of contamination will always be a concern, methods for verifying the true origin of zircons are crucial. Low-temperature thermochronological methods, such as fission tracks and (U-Th)/He, may shed light on the most recent thermal history of zircons[10, 22-26]. Unfortunately, such methods are time-consuming, destructive, and require crystals of a certain quality and size to get proper age determinations. An alternative method involves Raman spectroscopy, which allows for *in-situ* (~2 µm spatial resolution) characterization of the radiation damage to the zircon lattice[1, 27-31]. Experiments have shown that moderately radiation-damaged zircons reorganize their structure at >700°C on a timescale of hours to days[27, 32, 33]. This implies that zircons incorporated in a melt will anneal and show similar

crystallinity to the zircons that crystallized with the host rock, while the original U-Pb dates may be preserved due to low Pb-diffusion rates[16].

Because of the widespread geodynamic implications of inherited zircons, and the possibility for misinterpretation of contaminated grains as inherited, this paper aims to show how radiation damage measured through rapid and non-destructive Raman spectroscopy may remove uncertainties regarding sample contamination. Importantly, this approach can be used to revisit previously investigated samples to verify the findings. We first present a study of zircon U-Pb age and Raman spectroscopy analysis from an oceanic gabbro (Case 1, Mohn's Ridge, 73°N: Figure 1), and then we validate the method using a systematic study of inherited continental zircons from igneous rocks that formed during the opening of the Atlantic Ocean (Case 2, Gjallar Ridge, 65˚N: Figure 1).

Results And Discussion

Case 1: Precambrian zircons in mid-ocean ridge gabbro

A single gabbroic sample (GS16A-ROV6-016) was selected for zircon separation using ~10 kg of material. Based on a Raman spectroscopy screening before mounting of zircons in epoxy, 18 grains were selected for U-Pb isotope analysis using LA-ICP-MS. Eight grains show Pliocene U-Pb systematics with a mean weighted average $^{206}Pb/^{238}U$ age of 4.15 ± 0.13 Ma (MSWD = 1.2, n = 7) and has a characteristic low U (between 8 ppm and 64 ppm) and Th content (between 7 ppm and 72 ppm) and effective U concentrations (eU = U + Th) between 50 ppm and 75 ppm. One grain has markedly elevated U (606 ppm) and Th (711 ppm) yielding an effective U concentration of 1317 ppm. The grains are subhedral to euhedral and exhibit concentric and oscillatory zoning in cathodoluminescence images, indicating that the grains have crystallized in a melt. They show mean v3 (SiO_4) peak position of 1009.3 cm^{-1} and a range from 1009.0 cm^{-1} to 1009.6 cm^{-1}. The full width at half maximum (FWHM), corrected for spectral resolution, shows a mean of 1.95 and a range between 1.40 to 2.51 (Figure 2a). Ten grains have Precambrian U-Pb dates, with individual spot analysis yielding dates that range from 2724 Ma to 554 Ma ($^{206}Pb/^{238}U$ age <1500 Ma, $^{207}Pb/^{206}Pb$ age >1500 Ma). They have variable U (between 82 ppm and 541 ppm) and Th (between 53 ppm and 396 ppm) concentrations and show a linear shift of v3 (SiO_4) peak positions consistent with the accumulation of radiation damage because of alpha-decay (Figure 2a). Internal radiation doses were calculated for the Precambrian zircons (details in methods) and plot below a calibration curve for unannealed grains (Figure 2b).

We interpret the mean $^{206}Pb/^{238}U$ age of 4.15 ± 0.13 Ma to represent the crystallization of the mafic magma during plate separation, which is consistent with the sample position relative to the rift valley. The unexpected presence of Precambrian zircons in the young oceanic lithosphere requires a careful appraisal. A possible explanation is that these zircons were recycled from older crustal rocks in the mantle source e.g.,[2, 4]. Earlier reports of inherited zircons in mantle-derived rocks often assumed that their studied grains belonged to that specific sample, however, U-Pb dates alone do not rule out other

explanations. Another plausible explanation is that they are contaminants from sample processing. Experiments have shown that moderately radiation-damaged zircons completely reorganize their structure at 900°C at timescales of hours to days[32]. Consequently, grains that were incorporated in a mafic melt should show crystallinities similar to the young magmatic grains. The large spread in zircon v3 (SiO_4) peak positions ranging from 1007.8 cm^{-1} to 998.0 cm^{-1} and FWHM between 3.51 and 14.70 show that the older-than host rock grains have accumulated substantially more radiation damage than the young magmatic zircons (Figure 2a and b). The observations and data presented here demonstrate that the Precambrian zircons are contaminated from sample processing and not inherited zircons.

Case 2: Older-than host rock zircons in Cenozoic sills

To confirm that our approach allows distinction between contamination and true inherited zircons, we tested the Raman systematics in igneous rocks that formed during the opening of the Atlantic Ocean, and therefore are likely to contain inherited zircons of continental origin. In eighty-five zircons, both rims and interior sections were analyzed for U-Pb by LA-ICP-MS to compare internal age differences, resulting in 448 analytical spots on 215 grains. The two analyzed samples yielded mean weighted average $^{206}Pb/^{238}U$ ages of 54.21 ± 0.13 Ma (MSWD = 2.16; n = 46) and 55.57 ± 0.12 Ma (MSWD = 4.14; n = 63), analysis with over 2% uncertainty or discordance were excluded from the age calculations. This is within the uncertainty of previously reported weighted mean TIMS U-Pb ages of magmatic sills in the Vøring basin[34]. Seventy-nine zircons have dates between 80 Ma and 2200 Ma and twenty-four out of these display old-core young-rim. The zircons have mean and median U concentrations of 187 ppm and 151 ppm, respectively, and a range in U content from 12 ppm to 1430 ppm. The concentration of Th ranges from 5 ppm to 759 ppm and U/Th has a mean of 3.4 and a median of 3.3. The effective U concentration ranges from 16 ppm to 1764 ppm with a mean and median of 269 ppm and 205 ppm, respectively.

We studied 116 of the dated grains also by using Raman spectroscopy to investigate the effect of structural recovery of zircons included in the melt. Grains are atomically well-ordered with a mean v3 (SiO_4) peak position of 1008.2 cm^{-1} and a range from 1006.5 cm^{-1} to 1009.2 cm^{-1}. The full width at half maximum (FWHM), corrected for spectral resolution, shows a mean of 2.74, a median of 2.68, and a range between 0.51 to 5.12 (Figure 2c). Most grains are zoned regarding the FWHM as documented by multiple measurements on each grain. Cores generally display lower v3 (SiO_4) peak positions and higher eU compared with rims. The tight clustering of the zircon v3 (SiO_4) peak positions at ~1008 cm^{-1} and FWHM of ~2.8 show that the inherited grains have crystallinities comparable to the young magmatic zircons (Figure 2c). Most internal radiation doses calculated for the inherited zircons plot below a calibration curve for unannealed grains (Figure 2d) demonstrating that they have experienced annealing of the radiation damage after their formation. The calculated radiation doses for the young zircons exceed what can be ascribed to internal radiation doses purely by α-decay, suggesting internal tensional strain due to substitution[35] or rapid growth. We have calculated radiation damage dates (details in methods) for all spot analyzes, which are plotted against eU in Figure 3a.

Our finding of older-than host rock zircons in magmatic sills with crystallinity similar to the young magmatic grains (Figure 2c and d) demonstrates that all zircons share the same recent thermal history. The range of observed FWHM fits remarkably well with the expected range for the accumulation of radiation damage since approximately 55 Ma at a range of eU content from ~200 ppm to 1500 ppm (Figure 3b). In contrast, older grains that did not experience this annealing event would have accumulated radiation damage for longer periods and should show higher FWHM (i.e., following the trajectory in Figures 2c and d). As in case 1, such grains should therefore be considered foreign to the sample. We find that grains with over 800 ppm eU consistently yield radiation damage dates close to the magmatic age (Figure 2c and 3a), demonstrating the value of this approach for the identification of inherited zircons. Our results show that this applies to all grain morphologies, including those that display old core–old rims (Figure 4). Radiation damage dates for grains with lower than 800 ppm eU are variable (Figure 3a) and suggest that residual lattice distortion has not been fully annealed because eU strongly controlled the closure temperatures, a feature that has been suggested for the (U-Th)/He system in zircon e.g.,[36]. Alternatively, it may represent the analytical resolution of the method because higher eU leads to more drastic changes in the accumulation of radiation damage. From the contour lines in figure 3b, it is clear that small variations in the measured FWHM leads to drastic changes in the calculated radiation dates.

Implications for the interpretation of inherited zircons

The presence of continental zircons in oceanic rocks has long been considered an enigmatic feature owing to the sparse evidence of their actual origin. Because current practices for the identification of inherited zircons are based primarily on U-Pb dates, it is hampered by the fact that grains having old cores with rim dates similar to host-rock are rare. Our demonstration that the annealing of zircons in natural magmas may provide undisputed evidence for the existence of inherited materials is significant in at least two major respects. First, it provides a framework for the identification and interpretation of inherited zircons in a range of geological environments, such as mid-ocean ridges[2, 4], oceanic hot spots[5, 6], and island arcs[37, 38]. This approach is especially suited for young magmatic rocks where the age contrast between inherited and magmatic zircons may be large. Second, the method provides a means to revisit previously dated samples, potentially leading to the verification of disputed hypotheses. Implementation of this approach will improve our understanding of crustal recycling in the mantle and continental-influenced magmatism by removing the uncertainty related to the true origin of inherited material and may lead to a re-evaluation of current geodynamic models.

The fact that our findings are inconsistent with the presence of continental material in the shallow upper mantle beneath the Mohns Ridge has implications for understanding the mantle dynamics and warrants a discussion on why inherited zircons that appear elsewhere along the ridge segment are lacking here. Three contrasting possibilities must be evaluated: 1) recycling of continental material is localized to distinct regions of the mid-ocean ridges; 2) incorporation of continental material occurs at variable rates through time; 3) earlier proposed inherited zircons represent contamination. Considering the number of sites where old inherited zircons have been reported from the Mid-Atlantic Ridge (e.g., 64% of samples between 21°S and 42°N contained apparently inherited zircons[4]), such strong localization of continental

material along the mid-ocean ridge appears unlikely. In addition, the slow-spreading rate, proximity to the continental margin, and young age of the Norwegian-Greenland Sea are factors that should increase the likelihood of discovering a continental signature[4]. It is possible that the recycling of continental material in the oceanic mantle asthenosphere is less widespread than previously proposed and occurs in discrete pulses, but there are currently too few constraints to draw any firm conclusions. Another plausible explanation is that previously proposed inherited grains are contamination. Previous reports of inherited zircons along the mid-ocean ridge have focused on U-Pb dating of separated zircons, and in-situ studies have been unable to replicate the findings[39]. Failure to address the low-temperature history of the grains and a lack of in-situ confirmation, therefore, leaves significant uncertainty related to the interpretation of inherited zircons in the sub-oceanic mantle and beneath ocean islands. Consequently, the results from the two-step approach presented here raise intriguing questions regarding the nature and extent of continental recycling along the mid-ocean ridges and further research should be undertaken to confirm the validity of earlier claims.

Methods

Sample descriptions

Oceanic gabbro sample GS16A-ROV6-016 was collected using a remotely operated vehicle during a research cruise with G/O SARS in 2016 at a depth of 2449 mbsl at the Schulz Massif (73.7298N 7.5191E: Case 1: Figure 1). The rock is undeformed and comprises large plagioclase and pyroxene crystals which have been affected by various degrees of hydrothermal alteration. The subhedral to euhedral zircons have a mean length of 112 µm, a median length of 101 µm, and a range between 53 µm to 230 µm. Sector zoning and oscillatory zoning are visible in cathodoluminescence images (CL) and are interpreted to represent growth textures as the minerals crystallized from magma.

Dacite (13C-ROV6-5: 65.8958N 1.7944E) and trachydacite (13C-ROV7-1: 65.8979N 1.7846E) were sampled during a research cruise with the M/V Seabed Worker in 2013 at depths of 2205 mbsl and 2755 mbsl, respectively, at the Gjallar Ridge (Case 2: Figure 1). In the thin section, zircon occurs within feldspar and garnet phenocrysts, and as free crystals within the fine-grained matrix. Zircon, quartz, apatite, monazite, and FeTi-oxides are found as inclusions in garnet. The zircons are euhedral to subhedral, have a mean length of 216 µm, a median length of 170 µm, a mode of 119 µm, and range between 61 and 820 µm. Sector zoning and oscillatory zoning are visible in cathodoluminescence images (CL) and are interpreted to represent growth textures as the minerals crystallized from magma. Several grains display core-rim morphology and have characteristic rounded cores, which are both darker and lighter than their rim in CL images. No resorption or micro-porosity, which indicates alteration, was observed.

U-Pb geochronology

Approximately ten kg of gabbro and two to three kg of dacite/trachydacite were crushed by hand and put through a Wifley-shaking table, after which the magnetic minerals were removed using a Frantz magnetic

separator. The remaining material was run through a single heavy liquid step using diiodomethane to concentrate zircons. Grains were hand-picked and mounted in 25 mm epoxy blocks and polished to expose the zircons for further analysis. Mounts were then imaged in transmitted and reflected light using a Nikon LV100Pol polarizing microscope with a DS-Fi3 color camera, followed by backscatter and cathodoluminescence conducted using a Zeiss Supra 55VP SEM at the University of Bergen. Zircon parameters were measured using thresholding and particle counting in ImageJ.

U-Pb analysis of zircons was performed at Bergen Geoanalytical Facility at the University of Bergen using a 193 nm ArF excimer laser ablation system (RESOlution M-50 LR) coupled to an HR-SC-ICP-MS (Nu Instruments Attom ES) using parameters reported in Supplementary Material 1. The zircons were ablated for 30 s, after 15 s of blank measurement, using a 26 µm spot size, 5 Hz, and a fluence between 2 - 2.5 J/cm^2. The data were acquired in time-resolved peak-jumping pulse-counting mode with 1 point measured per peak for masses ^{202}Hg + ^{204}Pb + Hg, ^{206}Pb, ^{207}Pb, ^{208}Pb, ^{232}Th, ^{235}U, and ^{238}U. Because of the non-linear transition between the two counting modes in the ICP-MS, ^{238}U was calculated from ^{235}U when measured in attenuated mode (^{238}U counts = ^{235}U counts × 137.818) using a purpose-made python script.

Data reduction was done using Iolite 4 (v. 4.4.5) with the VizualAge UComPbine[40] data reduction scheme. Data reduction methodology follows Paton [41] and includes a correction for gas blank, laser-induced elemental fractionation of Pb and U, and instrument mass bias. Both blank counts and instrumental bias were corrected with an automatic spline function, while down-hole element fractionation was corrected using an exponential or exponential + line function. Common Pb correction was not applied to the data, only monitored. The remaining element fractionation and instrumental mass bias were corrected by normalization to the natural zircon reference material 91500[42]. For quality control, the zircon reference materials GJ1[43], Plešovice[44], and Mud Tank[45] were measured regularly and values are reported in Supplementary Material 1. The IsoplotR[46] program was used to generate weighted average and kernel density estimate (KDE) plots.

Measuring and evaluating zircon radiation damage in zircons

Raman spectra were recorded with a Jobin Yvon Labram-HR system equipped with an Olympus BX41 microscope, a Peltier-cooled charge-coupled device (CCD) detector, and 1800 grooves/mm diffraction grating. Excitation was performed using a 514 nm Ar-ion laser through a density filter (D = 0.3) and measurements were made using a 50x objective. Wavenumber calibration was performed on the 520.7 cm^{-1} band of a silicon wafer and the Rayleigh line. Background subtraction and peak fitting were done with the Fityk 1.3.1 program[47]. Peaks were fitted with a PseudoVoigt function and the peak shift position and width were determined for the v3 (SiO_4) band at 1008 cm^{-1}. Bandwidth was corrected for a measured spectral resolution of 2.0 - 2.5 cm^{-1} according to:

$$b = b_s \times \sqrt{1 - 2\left(\frac{s}{b_s}\right)^2}. (1)$$

where b is the corrected FWHM, b_s is the measured FWHM and s is the spectral resolution.

Radiation damage to the zircon lattice is evaluated by measuring the full-width half maximum (FWHM) of the v3 (SiO_4) peak position, which is a proxy for radiation damage. Crystals that have accumulated higher radiation doses (a factor of accumulation time and concentration of actinides) will have wider peaks with peak center position progressively lowered. By determining the U-Pb age, U and Th concentrations together with the measured FWHM of a single zircon, we can calculate the α-dose received by that grain according to[1, 48]:

$$D_\alpha = 8 \times \frac{C_U \times N_A \times 0.9928}{M_{238} \times 10^6} \times \left(e^{\lambda_{238} t} - 1\right) + 7 \times \frac{C_U \times N_A \times 0.0072}{M_{235} \times 10^6} \times \left(e^{\lambda_{235} t} - 1\right) + 6 \times \frac{C_{Th} \times N_A}{M_{232} \times 10^6} \times \left(e^{\lambda_{232} t} - 1\right). (2)$$

where C_U and C_{Th} are the concentration of U and Th (in ppm), N_A is Avogadro's number (6.022 x 10^{23}), M_{238}, M_{235} and M_{232} are the molecular weight of the isotopes, λ_{238}, $\lambda_{235,}$ and λ_{232} are the respective decay constants, and t is the time. Decay constants for ^{238}U, ^{235}U and ^{232}Th are 1.55125 x 10^{-10}, 0.98485 x 10^{-9} and 4.9475 x 10^{-11}, respectively.

A model calibration curve of unannealed zircons[1] allows us to calculate the zircon radiation damage age, which is the time required for that particular zircon to develop its observed radiation damage[28, 49]. We used the equation[28]:

$$FWHM = A\left[1 - exp^{(-B_{FWHM} D_{ed})}\right]. (3)$$

rearranged to:

$$D = \frac{\ln\left(1 - \frac{FWHM}{A}\right)}{-B}. (4)$$

to determine the radiation damage ages. A = is the asymptotically approached FWHM value of 35.64. B is related to the mass of material damaged per α-decay event calculated as 5.49 × 10− 19/g, and D is the equivalent damage dose determined from the U and Th contents. Reported radiation damage ages show geologically meaningful ages[50] and a similar age range as other low-temperature thermochronological

methods, such as zircon and apatite (U/Th)/He[31, 36]. The main difference being a consistent slightly older age determined by the radiation damage age method.

Declarations

Acknowledgments

This work was funded by the K.G. Jebsen Foundation with support from the Norwegian Petroleum Directorate. The authors thank A. Beinlich for suggestions and comments on earlier drafts of this manuscript.

Author Contributions

A.B. designed the study with input from H.H.S., L.E.R.P., and R.B.P. A.B. generated and interpreted the Raman data. L.E.R.P. generated geochronology data. R.B.P. secured funding for sample collection and analysis. A.B. wrote the paper with contributions from all co-authors.

Competing Interests statement

The authors declare no competing interests.

Data availability

The data of this study are available in supplementary tables.

References

1. Nasdala L*, et al.* Metamictisation of natural zircon: accumulation versus thermal annealing of radioactivity-induced damage. *Contributions to Mineralogy and Petrology*, **141**, 125-144 (2001)

2. Pilot J, Werner C-D, Haubrich F, Baumann N. Palaeozoic and Proterozoic zircons from the Mid-Atlantic Ridge. *Nature*, **393**, 676-679 (1998)

3. Skolotnev SG, Bel'tenev VE, Lepekhina EN, Ipat'eva IS. Younger and older zircons from rocks of the oceanic lithosphere in the Central Atlantic and their geotectonic implications. *Geotectonics*, **44**, 462-492 (2010)

4. Bea F*, et al.* Zircon xenocryst evidence for crustal recycling at the Mid-Atlantic Ridge. *Lithos*, **354-355**, 1-11 (2020)

5. Ashwal LD, Wiedenbeck M, Torsvik TH. Archaean zircons in Miocene oceanic hotspot rocks establish ancient continental crust beneath Mauritius. *Nature Communications*, **8**, 14086 (2017)

6. Torsvik TH*, et al.* A Precambrian microcontinent in the Indian Ocean. *Nature Geoscience*, **6**, 223-227 (2013)

7. Cheng H*, et al.* Jurassic zircons from the Southwest Indian Ridge. *Scientific Reports*, **6**, 26260 (2016)

8. Shellnutt JG, Lee T-Y, Chiu H-Y, Lee Y-H, Wong J. Evidence of Middle Jurassic magmatism within the Seychelles microcontinent: Implications for the breakup of Gondwana. *Geophysical Research Letters*, **42**, 207-210,215 (2015)

9. Xu Z, Zheng Y-F, Zhao Z-F. Zircon evidence for incorporation of terrigenous sediments into the magma source of continental basalts. *Scientific Reports*, **8**, 178 (2018)

10. Siebel W*, et al.* Prolonged mantle residence of zircon xenocrysts from the western Eger rift. *Nature Geoscience*, **2**, 886-890 (2009)

11. Zhang H-F*, et al.* Phanerozoic reactivation of the Archean North China Craton through episodic magmatism: Evidence from zircon U–Pb geochronology and Hf isotopes from the Liaodong Peninsula. *Gondwana Research*, **19**, 446-459 (2011)

12. Liu Y*, et al.* Continental and Oceanic Crust Recycling-induced Melt–Peridotite Interactions in the Trans-North China Orogen: U–Pb Dating, Hf Isotopes and Trace Elements in Zircons from Mantle Xenoliths. *Journal of Petrology*, **51**, 537-571 (2009)

13. Gao S*, et al.* Recycling lower continental crust in the North China craton. *Nature*, **432**, 892-897 (2004)

14. Robinson PT*, et al.* The origin and significance of crustal minerals in ophiolitic chromitites and peridotites. *Gondwana Research*, **27**, 486-506 (2015)

15. Yamamoto S*, et al.* Recycled crustal zircons from podiform chromitites in the Luobusa ophiolite, southern Tibet. *Island Arc*, **22**, 89-103 (2013)

16. Bea F, Montero P, Palma JFM. Experimental evidence for the preservation of U-Pb isotope ratios in mantle-recycled crustal zircon grains. *Scientific Reports*, **8**, 12904 (2018)

17. Kinny PD, Meyer HOA. Zircon from the Mantle: A New Way to Date Old Diamonds. *The Journal of Geology*, **102**, 475-481 (1994)

18. Borisova AY*, et al.* Zircon survival in shallow asthenosphere and deep lithosphere. *American Mineralogist*, **105**, 1662-1671 (2020)

19. Dickinson JE, Hess PC. Zircon saturation in lunar basalts and granites. *Earth and Planetary Science Letters*, **57**, 336-344 (1982)

20. Borisov A, Aranovich L. Zircon solubility in silicate melts: New experiments and probability of zircon crystallization in deeply evolved basic melts. *Chemical Geology*, **510**, 103-112 (2019)

21. Boehnke P, Watson EB, Trail D, Harrison TM, Schmitt AK. Zircon saturation re-revisited. *Chemical Geology*, **351**, 324-334 (2013)

22. Blondes MS, Reiners PW, Edwards BR, Biscontini A. Dating young basalt eruptions by (U-Th)/He on xenolithic zircons. *Geology*, **35**, 17-20 (2007)

23. Sutherland FL, Fanning CM. Gem-bearing basaltic volcanism, Barrington, New South Wales: Cenozoic evolution, based on basalt K–Ar ages and zircon fission track and U–Pb isotope dating. *Australian Journal of Earth Sciences*, **48**, 221-237 (2001)

24. Orme DA, Reiners PW, Hourigan JK, Carrapa B. Effects of inherited cores and magmatic overgrowths on zircon (U-Th)/He ages and age-eU trends from Greater Himalayan sequence rocks, Mount Everest region, Tibet. *Geochemistry, Geophysics, Geosystems*, **16**, 2499-2507 (2015)

25. Guenthner WR, Reiners PW, Ketcham RA, Nasdala L, Giester G. Helium diffusion in natural zircon: Radiation damage, anisotropy, and the interpretation of zircon (U-Th)/He thermochronology. *American Journal of Science*, **313**, 145-198 (2013)

26. Nasdala L*, et al.* Incomplete retention of radiation damage in zircon from Sri Lanka. *American Mineralogist*, **89**, 219-231 (2004)

27. Ginster U, Reiners PW, Nasdala L, Chanmuang N C. Annealing kinetics of radiation damage in zircon. *Geochimica et Cosmochimica Acta*, **249**, 225-246 (2019)

28. Palenik CS, Nasdala L, Ewing RC. Radiation damage in zircon. *American Mineralogist*, **88**, 770-781 (2003)

29. Nasdala L, Irmer G, Wolf D. The degree of metamictization in zircon; a Raman spectroscopic study. *European Journal of Mineralogy*, **7**, 471-478 (1995)

30. Geisler T, Pidgeon RT, Van Bronswijk W, Pleysier R. Kinetics of thermal recovery and recrystallization of partially metamict zircon : a Raman spectroscopic study. *European Journal of Mineralogy*, **13**, 1163-1176 (2001)

31. Härtel B, Jonckheere R, Wauschkuhn B, Ratschbacher L. The closure temperature(s) of zircon Raman dating. *Geochronology*, **3**, 259-272 (2021)

32. Ewing RC, Meldrum A, Wang LM, Weber WJ, Corrales LR. *Radiation Effects in Zircon*. J M Hanchar and P W O Hoskin: United States, 2003.

33. Widmann P, Davies JHFL, Schaltegger U. Calibrating chemical abrasion: Its effects on zircon crystal structure, chemical composition and UPb age. *Chemical Geology*, **511**, 1-10 (2019)

34. Svensen H, Planke S, Corfu F. Zircon dating ties NE Atlantic sill emplacement to initial Eocene global warming. *Journal of the Geological Society*, **167**, 433-436 (2010)

35. Kempe U*, et al.* Substitution-induced internal strain and high disorder in weakly radiation damaged hydrothermal zircon from Mt. Malosa, Malawi. *European Journal of Mineralogy*, **30**, 659-679 (2018)

36. Hueck M, Dunkl I, Heller B, Stipp Basei MA, Siegesmund S. (U-Th)/He Thermochronology and Zircon Radiation Damage in the South American Passive Margin: Thermal Overprint of the Paraná LIP? *Tectonics*, **37**, 4068-4085 (2018)

37. Tapster S, Roberts NMW, Petterson MG, Saunders AD, Naden J. From continent to intra-oceanic arc: Zircon xenocrysts record the crustal evolution of the Solomon island arc. *Geology*, **42**, 1087-1090 (2014)

38. Rojas-Agramonte Y*, et al.* Ancient xenocrystic zircon in young volcanic rocks of the southern Lesser Antilles island arc. *Lithos*, **290-291**, 228-252 (2017)

39. Hellebrand E, Möller A, Whitehouse M, Cannat M. Formation of oceanic zircons. *Geochim Cosmochim Acta*, **71**, A391-A391 (2007)

40. Chew DM, Petrus JA, Kamber BS. U–Pb LA–ICPMS dating using accessory mineral standards with variable common Pb. *Chemical Geology*, **363**, 185-199 (2014)

41. Paton C*, et al.* Improved laser ablation U-Pb zircon geochronology through robust downhole fractionation correction. *Geochemistry, Geophysics, Geosystems*, **11**, (2010)

42. Wiedenbeck M*, et al.* Three Natural Zircon Standards for U-Th-Pb, Lu-Hf, Trace Element and Ree Analyses. *Geostandards and Geoanalytical Research*, **19**, 1-23 (1995)

43. Jackson SE, Pearson NJ, Griffin WL, Belousova EA. The application of laser ablation-inductively coupled plasma-mass spectrometry to in situ U–Pb zircon geochronology. *Chemical Geology*, **211**, 47-69 (2004)

44. Sláma J*, et al.* Plešovice zircon — A new natural reference material for U–Pb and Hf isotopic microanalysis. *Chemical Geology*, **249**, 1-35 (2008)

45. Horstwood MSA*, et al.* Community-Derived Standards for LA-ICP-MS U-(Th-)Pb Geochronology – Uncertainty Propagation, Age Interpretation and Data Reporting. *Geostandards and Geoanalytical Research*, **40**, 311-332 (2016)

46. Vermeesch P. IsoplotR: A free and open toolbox for geochronology. *Geoscience Frontiers*, **9**, 1479-1493 (2018)

47. Wojdyr M. Fityk: a general-purpose peak fitting program. *Journal of Applied Crystallography*, **43**, 1126-1128 (2010)

48. Murakami T, Chakoumakos BC, Ewing RC, Lumpkin GR, Weber WJ. Alpha-decay event damage in zircon. *American Mineralogist*, **76**, 1510-1532 (1991)

49. Pidgeon RT. Zircon radiation damage ages. *Chemical Geology*, **367**, 13-22 (2014)

50. Jonckheere R, Heinz D, Hacker BR, Rafaja D, Ratschbacher L. A borehole investigation of zircon radiation damage annealing. *Terra Nova*, **31**, 263-270 (2019)

Figures

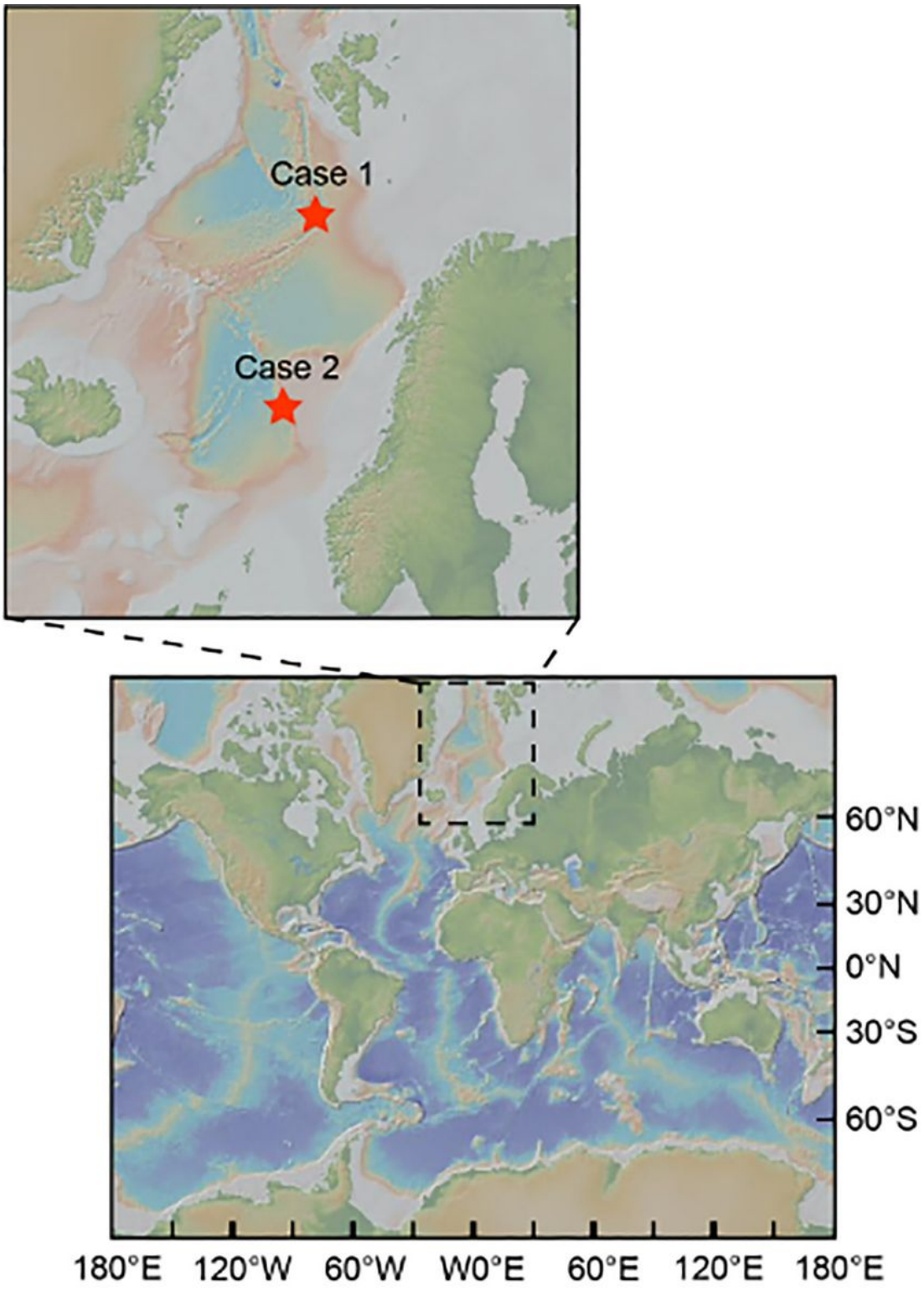

Figure 1

Geographic overview over the study area. Maps were created using GeoMapApp (www.geomapapp.org).

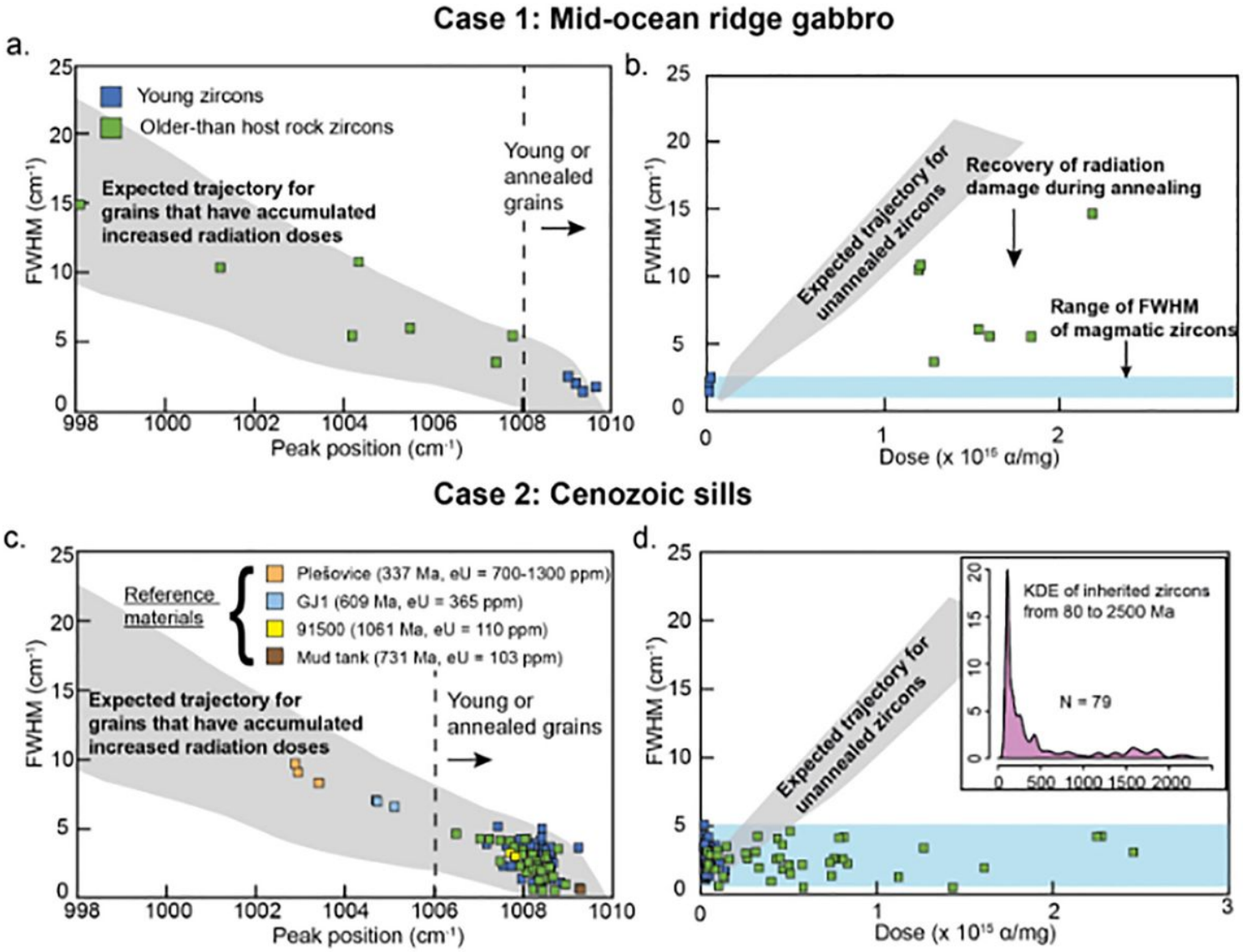

Figure 2

Evaluation of radiation damage of single zircon grains. a,c. Full width at half maximum (FWHM) vs peak position of the v3 (SiO_4) stretching band. b,d. FWHM vs α-dose for young and inherited zircons. Data for unannealed zircons from Nasdala et al. 2001. The vertical axis on the inset in figure d is based on histograms with a bandwidth of 40 Ma.

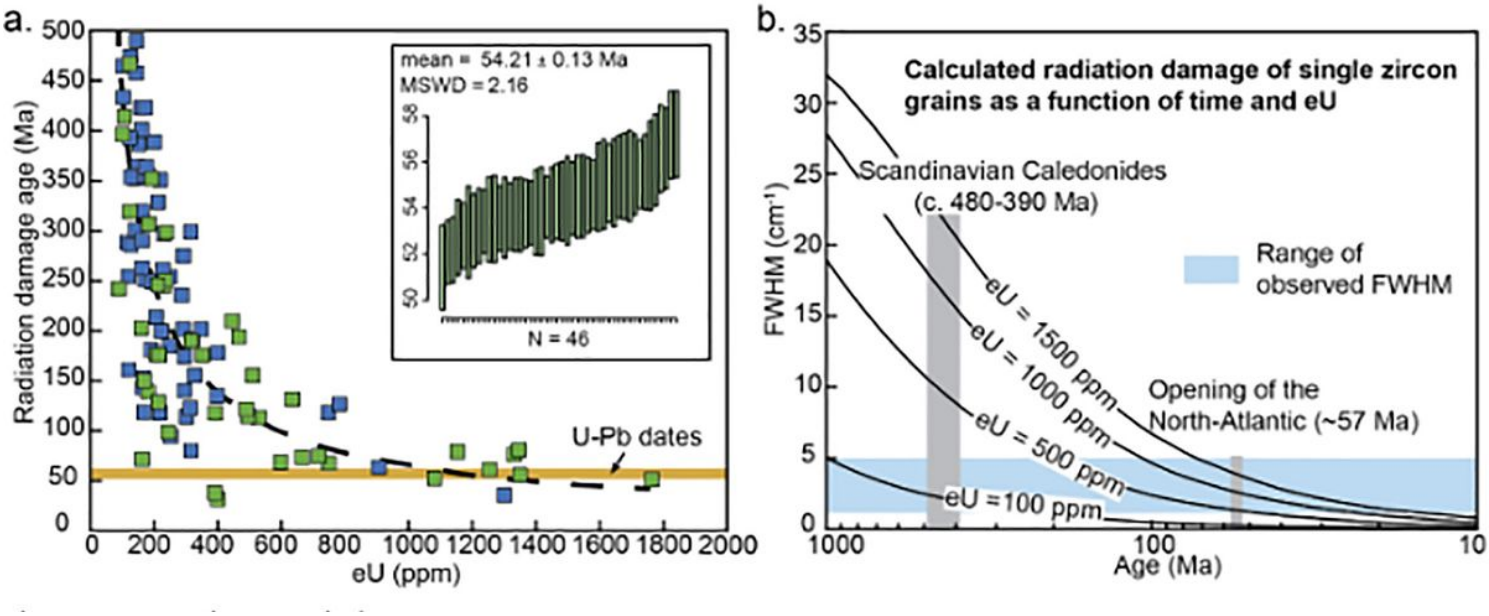

Figure 3

Calculation of radiation damage age. a. Calculated radiation damage age vs eU-content. Legend is the same as in figure 2. Inset shows the mean weighted average U-Pb age of sample 13C-ROV6-5. b. Evolution of radiation damage, measured as FWHM, of single zircon grains at different eU-content calculated using a U/Th of 3.4. The blue band shows the range of observed FWHM of all analyzed zircons.

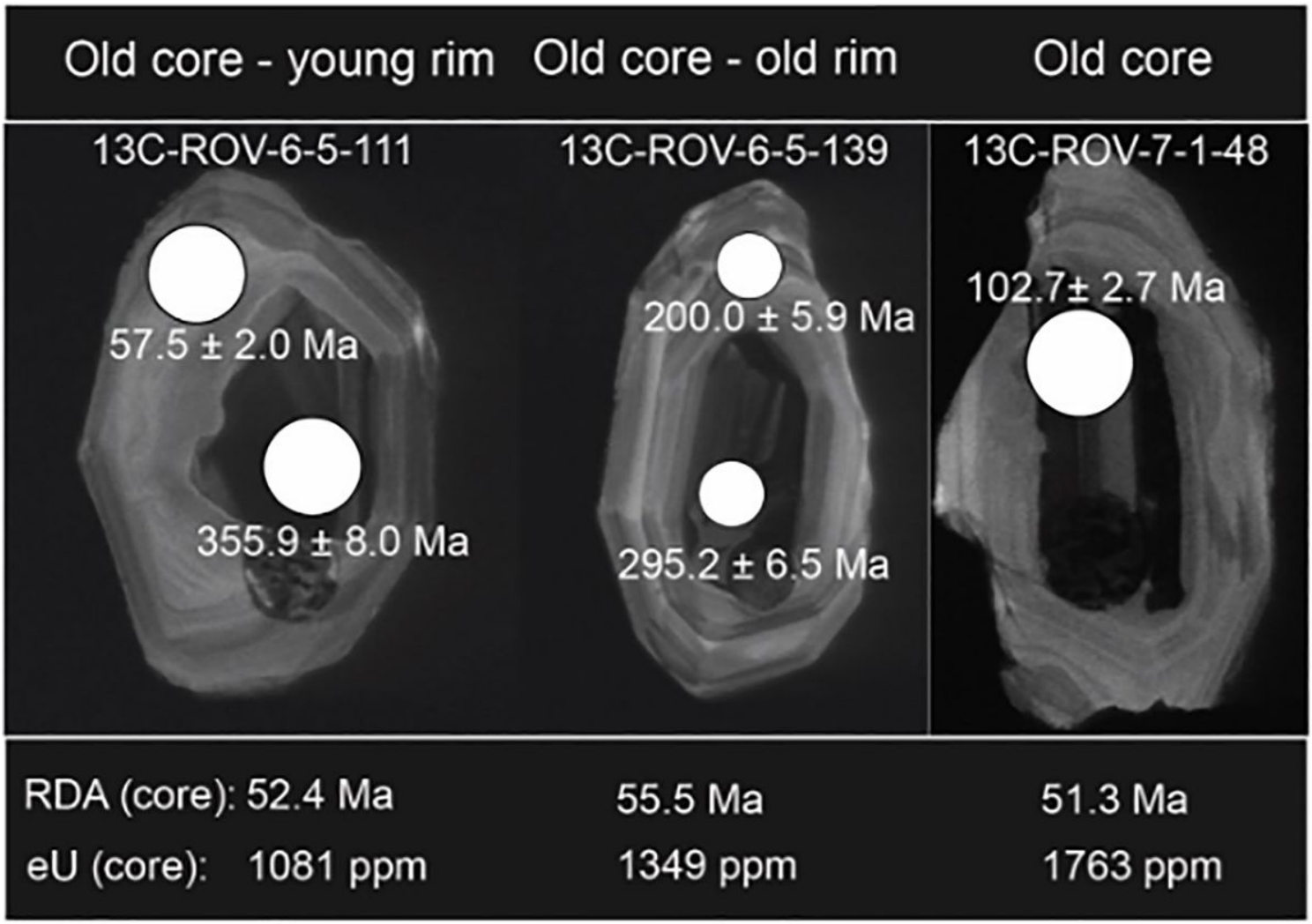

Figure 4

Cathodoluminescence images of selected zircons. Radiation damage age (RDA) of three morphologically different zircons. Scale is given by spot size (24 µm).

Supplementary Files

This is a list of supplementary files associated with this preprint. Click to download.

- SupplementaryTable2.xlsx
- SupplementaryMaterial1.docx
- SupplementaryTable1.xlsx